

---

# Satellite-Borne Measurements of Middle-Atmosphere Temperature [and Discussion]

J. J. Barnett and S. A. Bowhill

*Phil. Trans. R. Soc. Lond. A* 1987 **323**, 527-544

doi: 10.1098/rsta.1987.0103

---

## Email alerting service

Receive free email alerts when new articles cite this article - sign up in the box at the top right-hand corner of the article or click [here](#)

---

To subscribe to *Phil. Trans. R. Soc. Lond. A* go to: <http://rsta.royalsocietypublishing.org/subscriptions>

---

## Satellite-borne measurements of middle-atmosphere temperature

BY J. J. BARNETT

*Department of Atmospheric Physics, Clarendon Laboratory, University of Oxford,  
Oxford OX1 3PU, U.K.*

Satellites were first used to measure middle-atmosphere temperatures in the early 1960s. There has been steady progress towards the present position where we have routine observations of the whole stratosphere with 10–15 km vertical resolution by operational satellites, and where experimental instruments provide data as high as the mesopause, with 3 km vertical resolution in some cases. Vertical-viewing geometry is used in the simplest instruments, but limb viewing gives some advantages and has been exploited during the last decade. Measurements of the temperature field as a function of pressure allow the determination of geopotential height, hence of motions. The most complete geographical and temporal coverage is obtained by instruments that sense thermal emission, either in the infrared or the microwave. However, measurements of atmospheric infrared absorption from solar occultation, and of pressure scale height from measurements of solar scattering by air molecules, are also used to determine temperature. The paper outlines the present state of the art and will attempt to show how well we can hope to do in the future.

### 1. INTRODUCTION

Atmospheric physics and meteorology were among the first beneficiaries of artificial satellites, and by the early 1960s pictures in the visible region of the weather were being made operationally. Measurements were made of the middle atmosphere at an early stage, because the simplest kind of temperature sounding radiometer, one that measures emission from the whole  $\nu_2$  carbon dioxide band, measures primarily the low stratospheric Planck function.

Observing methods can be classified on the basis of geometry into the following.

(a) Those that view vertically or within about  $60^\circ$  of the vertical; they rely on geometry to select the measurement location horizontally, but on spectroscopy to determine the pressure level. These instruments typically scan across the satellite track to obtain complete global coverage with a horizontal resolution of a few tens of kilometres.

(b) Those that view along a limb path. They also use geometry to select the vertical location of the measurement, although spectroscopy is still a crucial aspect of the instrument design and data interpretation. Limb-viewing measurements necessarily have a resolution no better than a few hundred kilometres along the view direction. They can currently be divided into emission, occultation and pressure scale-height determination.

Satellite heights are normally in the 350–1000 km range, the former extreme being used for short-duration missions such as Spacelab where orbital decay is not a problem, whereas the latter is used by operational meteorology satellites where the swaths for vertical viewing imagers and sounders need to adjoin at the equator without excessive zenith angles. Low orbital height is an advantage for limb sounders, because fine vertical resolution is easier to achieve, but for a mission of one or more years' duration, a height of at least 500 km is needed to obtain a

[ 7 ]

sufficiently small orbit decay rate. The upper-atmosphere research satellite, described in §6, will be at 600 km nominal height, yet will still need periodic boosting to maintain this.

Table 1 lists the known instruments that have made, or will make, significant middle atmosphere temperature measurements. In the case of vertical sounders the main stream of development has been aimed at tropospheric weather forecasting, and any benefit for the

TABLE 1. SATELLITE INSTRUMENTS THAT MEASURE MIDDLE ATMOSPHERE TEMPERATURE

|                        |            |                  | vertical emission sensing                                      |   |
|------------------------|------------|------------------|--|---|
| <i>Tiros</i> 7...      | 1963–      | MRIR             | 1 temperature channel radiometer                               |   |
| <i>Nimbus</i> 2–3      | 1966–9     | MRIR             | low stratosphere   |   |
| <i>Nimbus</i> 3–4      | 1969–70    | SIRS             | grating spectrometer; low and mid-stratosphere                 |   |
| <i>Nimbus</i> 3–4      | 1969–70    | IRIS             | Michelson interferometer; low and mid-stratosphere             |   |
| <i>Nimbus</i> 4        | 1970       | SCR <sub>1</sub> | gas modulation: whole stratosphere                             |   |
| NOAA 2–5               | 1972–76    | VTPR             | radiometer; low stratosphere                                   |   |
| <i>Nimbus</i> 5        | 1972       | ITPR             | radiometer; low stratosphere                                   |   |
| <i>Nimbus</i> 5        | 1972       | SCR <sub>2</sub> | gas modulation; whole stratosphere                             |   |
| <i>Nimbus</i> 6        | 1975       | HIRS             | radiometer; low stratosphere                                   |   |
| <i>Nimbus</i> 6        | 1975       | PMR              | gas modulation; upper stratosphere and mesosphere              |   |
| <i>Tiros-N</i> ,       | 1978,      | { HIRS/2         | radiometer; low stratosphere                                   |   |
| NOAA 6,                | 1979–      |                  | MSU  | microwave radiometer; low stratosphere      |
| 7, 8, 9, 10...         | 86         |                  | SSU  | gas modulation; mid- and upper stratosphere |
| GOES 4...              | 1980–      | VAS              | geostationary; low stratosphere                                |   |
| DMSP                   | 1977–      | MFR              | radiometer; low stratosphere                                   |   |
| <i>Meteor</i> series   | late 1970s |                  | spectrometer and interferometer; low stratosphere              |   |
| <i>Meteor-2</i> series | late 1970s |                  | radiometer; low stratosphere (operational)                     |   |
|                        |            |                  | limb emission sensing  |   |
| <i>Nimbus</i> 6        | 1975       | LRIR             | radiometer; stratosphere and low mesosphere                    |   |
| <i>Nimbus</i> 7        | 1978       | LIMS             | radiometer; stratosphere and low mesosphere                    |   |
| <i>Nimbus</i> 7        | 1978       | SAMS             | gas modulation; stratosphere and mesosphere                    |   |
|                        |            |                  | limb Rayleigh solar scattering                                 |   |
| SME                    | 1981       |                  | visible spectrometer; upper stratosphere                       |   |
|                        |            |                  | solar occultation  |   |
| Spacelab 3             | 1985       | ATMOS            | Michelson interferometer; strato-, meso- and thermosphere      |   |
|                        |            |                  | future   |   |
| NOAA → J               |            | HIRS/2           | ssu and msu (ssu not on all satellites)                        |   |
| NOAA K...              | 1991       | AMSU and HIRS/2  | vertical microwave radiometer; whole stratosphere              |   |
| UARS                   | 1991       | ISAMS            | limb sounder; gas modulation; strato- and mesosphere           |   |
| UARS                   | 1991       | CLAES            | limb sounder; Fabry–Perot spectrometer; strato- and mesosphere |   |
| UARS                   | 1991       | HRDI             | Fabry–Perot interferometer; Doppler widths                     |   |
| UARS                   | 1991       | WINDII           | Michelson interferometer; Doppler widths                       |   |
| Spacelab               | 1990/1–    | ATMOS            | periodic reflights of short duration                           |   |

Abbreviations not in the text: MRIR, medium-resolution infrared radiometer; SIRS, satellite infrared spectrometer; MFR, multifilter radiometer; VAS, visible infrared spin scan radiometer atmospheric sounder.

middle atmosphere resulted partly because the low and mid-stratospheric channels could help to improve temperature retrievals in the troposphere, and because the extra stratospheric channels could be added at relatively little additional cost. The infrared interferometer spectrometers (IRIS) were in a different category, being survey-type instruments aimed at studying and checking our knowledge of the infrared spectrum. They were Michelson interferometers, and with their limited ( $2.8$  or  $5\text{ cm}^{-1}$ ) resolution they could obtain vertical profiles of temperature and some species in the low and mid-stratosphere. Other IRIS instruments went to Mars in 1971 on *Mariner 9*, and to Jupiter, the Jovian satellites, Saturn, Titan and Uranus on

the *Voyager* spacecraft (Hanel 1983). It is hoped that one will reach and make observations of Neptune in 1989.

The selective chopper radiometers (SCR) and the pressure modulator radiometer (PMR) were built specifically to sound temperature in the middle atmosphere. This required the development of a new form of radiometer employing gas-correlation spectroscopy to achieve adequate spectral resolution. This line of evolution finally merged with that aimed at weather forecasting, with the *Tiros*† operational vertical sounder (TOVS) set of sounders on the present *Tiros-N* satellites. The TOVS comprises the HIRS/2 (high-resolution infrared radiation sounder), MSU (microwave sounder unit) and SSU (stratospheric sounder unit), which together give weighting functions that sound temperature up to about 45 km altitude.

Limb-emission sounders were developed to obtain better vertical resolution and because they made constituent sounding possible for many additional species (Russell, this symposium; Taylor & Dudhia, this symposium). However, the opacity of the troposphere limits the lower altitude for limb measurements at all wavelengths to about 10 km. Occultation instruments for observing constituents, notably ozone, had been flown in the 1960s and 1970s, but the ATMOS was the first to measure temperature, and represented a large step forward in technology. Solar occultation gives geographical coverage that is poor compared with emission measurements with just two profiles per orbit at sunrise and sunset. However, the intensity of the radiation source enables measurements to be extended to greater heights, and in this case to be related to numerous other quantities measured simultaneously.

The final measurement category is the determination of pressure scale height, as is performed by the Solar Mesosphere Explorer (SME). The visible sunlight scattered by air molecules is measured and gives the relative pressure as a function of height, from which the temperature profile can be calculated.

All temperature sounders need to observe radiation scattered, absorbed or emitted by molecules of known mixing ratio. This is oxygen in the case of microwave sounders, and carbon dioxide (plus some tropospheric contribution from nitrous oxide) for the infrared sounders. For limb-viewing instruments these measurements not only yield temperature, but also enable density or pressure determination, so that the constituent measurements can be reduced to mixing ratios. In some cases, as shown in §2, the absolute height scale is poorly known from the satellite systems, and this pressure determination is essential as it is the vertical coordinate for the temperature measurement.

## 2. VERTICAL SOUNDING

The equation of radiative transfer gives the radiation measured at a satellite viewing through a non-cloudy aerosol-free atmosphere in terms of transmission to the satellite,  $\tau$ , and Planck function,  $B$ , as

$$I = \int_{\tau_0}^1 B d\tau + \tau_0 B_0, \quad (1)$$

where  $\tau_0$  is the transmission to the surface (assumed black) and  $B_0$  is the Planck function at the surface. In the case of a vertical path to the satellite, it is convenient to transform to a height-like

† *Tiros* is an abbreviation for television and infrared observations satellite.

variable  $z$ , which is most conveniently pressure scale height ( $-\ln(p/p_0)$ , where  $p$  is pressure and  $p_0$  is surface pressure). This gives

$$I = \int_{z_0}^{\infty} B(z) \frac{d\tau}{dz} dz + \tau_0 B_0; \quad (2)$$

$d\tau/dz$  is normally a bell-like function and is known as the weighting function. Figure 1 gives weighting functions for the main temperature sounding channels of the rovs. The surface term  $\tau_0 B_0$  is normally included as an additional element in the discretized weighting function,

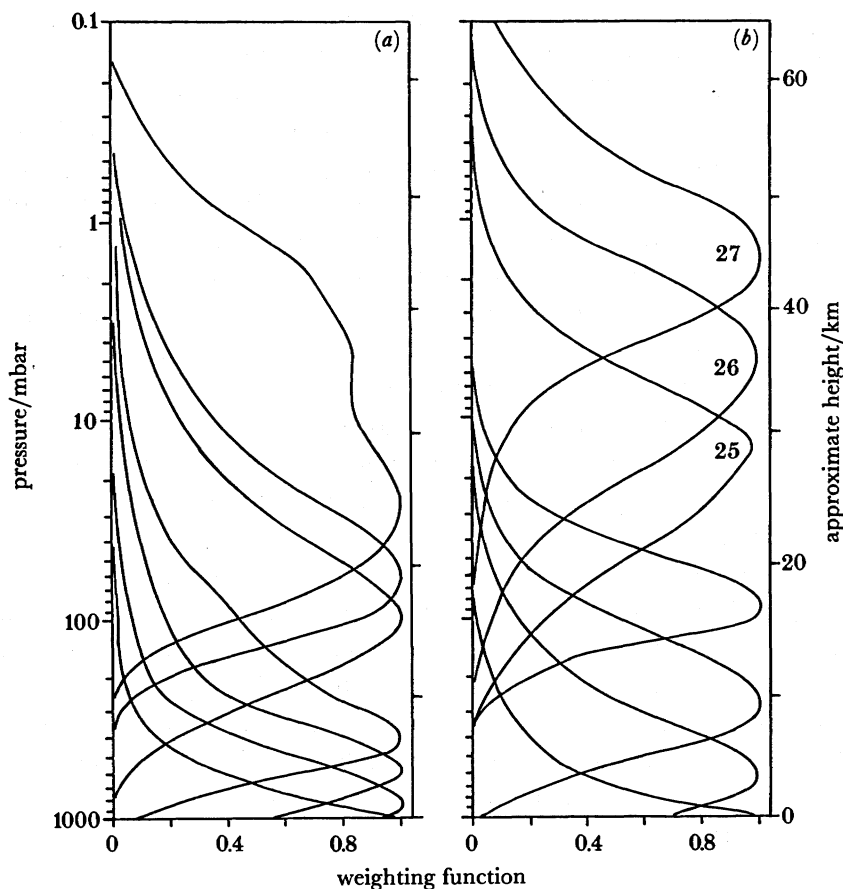


FIGURE 1. Weighting functions of (a) the HIRS/2, and (b) SSU (upper 3 curves) and MSU (lower 4 curves) sounders on the *Tiros-N* operational weather satellites. The weighting functions have been normalized to maximum values of unity. Only the carbon dioxide  $15 \mu\text{m}$  band channels are shown for the HIRS/2. The numbering of the SSU channels (25, 26, 27) corresponds to results given for them in figure 5b.

although it is normally zero for stratospheric weighting functions. The transmission  $\tau$  depends upon the spectral properties of the gas within the wavenumber limits observed. Up to about 50 km for the  $\nu_2$  carbon dioxide band (which is near  $667 \text{ cm}^{-1}$  or  $15 \mu\text{m}$ ), Lorentz broadening dominates the line shape. This is primarily pressure dependent, consequently weighting functions are normally specified in pressure coordinates, and are temperature dependent to a small extent because of the variation with temperature of line width and strength. On a height scale they would move bodily up or down, according to surface pressure, and would depend more



on temperature because the hydrostatic relation that interrelates the pressure and height scales also involves temperature.

If the viewing direction is moved away from the nadir by angle  $\theta$  relative to the local vertical in the atmosphere, the weighting functions will move upwards because of limb darkening. Where  $\theta$  is small, the effect is equivalent to multiplying the mixing ratio of the gas by  $\text{cosec } \theta$ . For larger angles this is still correct, except that  $\theta$  varies significantly with height. For still larger angles, approaching limb viewing, the vertical variation of  $\theta$  will vary significantly in pressure coordinates depending on the temperature profile, so introducing a further temperature dependence of the weighting function.

In practice, weighting functions are calculated and hence parametrized by elaborate spectral calculations that take into account all of these effects, so that they need not be treated individually. The result, however, is that the problem is no longer perfectly linear, and it is necessary to linearize about a mean Planck function profile, and use a deviation weighting function to allow for departures.

The HIRS/2 sounder has weighting functions (figure 1) very similar to the earlier operational sounders, such as the VTPR (vertical temperature profile radiometer). Much fundamental research was performed with these measurements, and this forms the basis of a substantial body of our present understanding of the low and mid-stratosphere.

The instruments described so far have a spectral resolution of a few wavenumbers, and the highest altitude weighting functions are obtained with passbands centred on the carbon dioxide band centre at about  $667 \text{ cm}^{-1}$ . Higher weighting functions are obtainable by selecting emission from near or at the centres of individual spectral lines. To select part of a single line would be difficult experimentally and would necessitate a very low noise detection system. However, by using a cell of carbon dioxide as a filter, oscillating its pressure (or chopping between two cells containing different pressures), and measuring the component of radiation incident on the detector at the chopping frequency, it is possible to measure emission from chosen parts of atmospheric lines. In addition the measurement is summed over all lines in the overall instrument band pass (e.g. the entire gas band), selecting in each case the portion of the line with about the same opacity. This is known as gas-correlation spectroscopy, and is described in detail by Taylor (1983). The opacity sensed depends upon the mean cell pressure, so by having different cells it is possible to obtain weighting functions at various heights. The principle was exploited in the *Nimbus 4* and *5* SCRS (which were quite different from each other in design), the *Nimbus 6* PMR and the *Tiros-N* series SSUS. The SCRS chopped between cells at different pressures, but this method is subject to errors caused by minor differences between the cells, limiting the maximum weighting function height to about 45 km. The PMR and SSUS use a single cell whose pressure is caused to oscillate at about 40 Hz by a piston suspended by diaphragm springs. This eliminates balance problems, and permits measurements to a much higher altitude.

The *Nimbus 6* PMR has two channels (pressure modulators), and when viewing vertically they have weighting functions peaking in the upper mesosphere. Taking a linear combination (essentially a difference) leads to a peak 15–20 km broad centred at about 80 km. Cell pressures of about 1 mbar† are necessary giving lines that are mainly Doppler broadened and only about  $0.001 \text{ cm}^{-1}$  wide, hence implying an effective spectral resolution of about  $10^6$ . The weighting

† 1 mbar =  $10^2$  Pa.

function peak is much broader than can be obtained in the stratosphere and troposphere because Doppler broadening is not pressure sensitive; this also leads to greater temperature dependence of the weighting functions. Any tilt of the viewing direction along the satellite velocity vector introduces a Doppler shift that causes the spectral lines in the cell to move relative to those in the atmosphere, and the weighting functions to move down. This was exploited in the PMR by including a mechanism to scan  $\pm 15^\circ$  forwards and backwards, causing the weighting functions to scan vertically between about 40 and 80 km. Each scan cycle took 96 s, and was timed to achieve field of view compensation, giving measurement profiles about  $6^\circ$  latitude apart. The 'Doppler scan' principle of the PMR is sometimes taken to be just limb darkening, but they act in opposite directions. The limb-darkening effect at the end of the scan is minor ( $\operatorname{cosec} 15^\circ = 1.036$ ). In contrast, the relative velocity for  $15^\circ$  tilt is about  $1.8 \text{ km s}^{-1}$ , corresponding to about 6 Doppler line half-widths.

The stratospheric sounder unit component of the TOVS uses three cross-track scanning pressure modulators to obtain stratospheric weighting functions. Technical details were given by Miller *et al.* (1980). Stratospheric channels were included in the TOVS both to enable more accurate tropospheric retrieval and to provide stratospheric fields that it was believed would become increasingly important in forecasting. Limb darkening causes problems with mapping of measurements of cross-track scanning instruments. In the case of the TOVS, away from nadir, radiances corresponding to the nadir weighting functions are obtained from those measured by linear combination, by using precalculated regression coefficients. All radiances are now for the same level, and can be mapped and then retrieved. Limb darkening has been exploited in the case of the SSU by Nash (1987), who used linear combinations of the weighting functions at  $5^\circ$  and  $35^\circ$  scan angles to synthesize narrow peaks higher than those of the contributing weighting functions (up to about 0.5 mbar). These combination weighting functions are applicable to zonal means and features where there is a zero or linear trend across the scan width. However, subtle effects can arise from solar tides because the observations are at local times that systematically change across the scan.

The weighting functions given in figure 1 show clearly that vertical-sounder measurements are well suited to the determination of temperature to a vertical resolution of 10–15 km. Many applications require a result at a finer resolution, and it is necessary to employ additional constraints, typically requiring the profile to be statistically like the known atmosphere. Given an *a priori* or 'first guess' Planck function profile  $B_0$ , a corresponding radiance  $I_0$ , a covariance  $S$  of  $B_0$ , a weighting-function matrix  $K$  and an error covariance  $E$  of the observation, the observation and *a priori* profiles can be combined optimally to give an estimate of the Planck function  $\hat{B}$

$$\hat{B} = B_0 + SK^T (KSK^T + E)^{-1} (I - I_0). \quad (3)$$

This approach is mathematically equivalent to multiple regression of a set of radiances against the corresponding Planck function profiles that have mean and covariance  $B$  and  $S$ . In the case of the TOVS data, as reduced by the Meteorological Office, only layer-mean temperatures are derived for a relative small number of layers, on the basis that this represents the full information content of the measurements. Retrieval theory for both vertical and limb sounding was described in detail by Rodgers (1976).

### 3. LIMB-EMISSION SOUNDING

The *Nimbus 6* limb radiance inversion radiometer (LRIR) was the first orbiting limb-emission temperature sounder. It used a large cryostat with solid methane and solid ammonia to cool the detectors and part of the optics to about 63 K. This limited its life to 7 months. The vertical field of view was 2 km, and the scan time was 2 s. In addition to measuring emission from carbon dioxide for temperature and pressure-level determination, the LRIR sounded ozone and water vapour.

*Nimbus 7* carried both an improved version of the LRIR, known as the limb infrared monitor of the stratosphere (LIMS), and the stratospheric and mesospheric sounder (SAMS). The LIMS and LRIR were described by Gille *et al.* (1980), and the LIMS, by Gille & Russell (1984). Improvements of the LIMS over the LRIR were the addition of nitric acid and nitrogen dioxide channels; the scan time was increased to 12 s. The LRIR and LIMS both used two channels to sound temperature and for determination of tangent point pressure. Both were in the  $\nu_2$  carbon dioxide band, one being sensitive to the band centre (*ca.* 645–673  $\text{cm}^{-1}$ ) and the other to the whole band (*ca.* 595–739  $\text{cm}^{-1}$ ).

The SAMS measured emission from carbon dioxide, together with nitrous oxide, methane, carbon monoxide, water vapour and nitric oxide. The instrument was described by Drummond *et al.* (1980), and some of the results by Barnett *et al.* (1985), Jones & Pyle (1984), Barnett & Corney (1984) and Taylor (this symposium). The SAMS employed gas-correlation techniques to achieve high spectral resolution, and consequently radiation could be separated into two components:

(a) that from just the very strong part of the spectrum near the centre of the main carbon dioxide band near 667  $\text{cm}^{-1}$  plus the centres of lines away from the band centre (two such channels sensitive to different degrees of opacity were included);

(b) that from the weaker part of the band, excluding strong line centres.

As shown in §3.1, the inclusion of channels measuring emission from different opacities is necessary for pressure and temperature determination.

#### 3.1. Information content of limb-emission measurements

The physical principles of emission limb sounder retrieval in the infrared were given by Gille & House (1971). They showed that by using two channels located in regions of different opacity, it is possible to deduce the temperature profile as a function of pressure, from radiance profiles obtained as functions of relative height.

The *Nimbus 7* satellite has attitude control that was relatively poor by current standards, and had absolute knowledge of roll angle corresponding to a few tens of kilometres at the limb. The high satellite altitude of 950 km was a contributing factor. The LIMS and SAMS relied on the assumption that the roll angle would change smoothly and sufficiently slowly so the relative heights of the field of view during vertical scans would be known to a fraction of a kilometre (after allowing for slow drifts). Thus radiance profiles could be obtained against relative height as a vertical coordinate. The SAMS had a typical scan time of 16 s (programmable) whereas the LIMS scanned in 12 s.

Figure 2 gives schematic weighting functions for a sounder with a narrow vertical field of view when viewing tangent levels that are at fixed pressure levels (weighting functions for viewing at fixed height levels are quite different and beyond the scope of this treatment). The



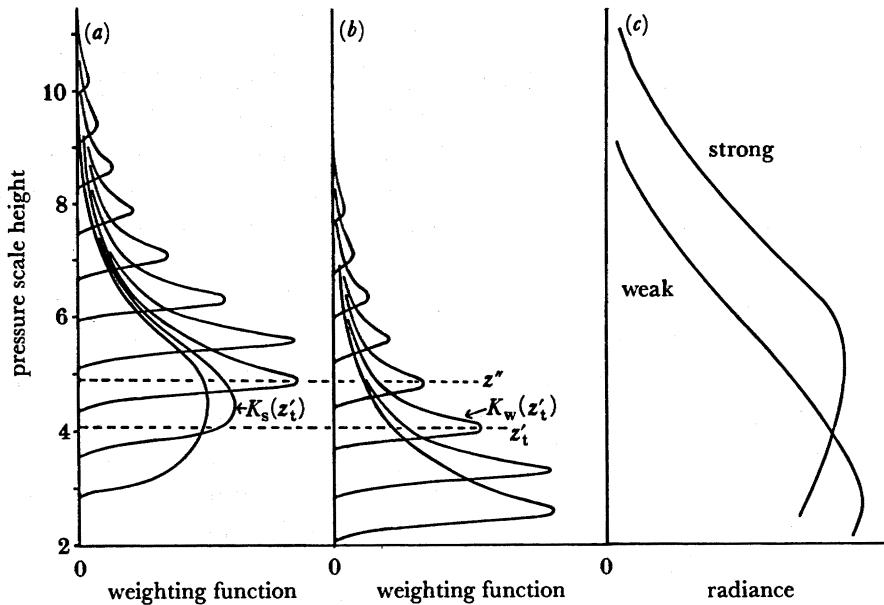


FIGURE 2. Weighting functions and measured radiance for a hypothetical infrared limb sounder with a 2 km wide field of view, and with two channels sounding at frequencies of (a) strong and (b) weak absorption. The radiance is shown in (c). The vertical scale is pressure scale height (one pressure scale height is approximately equivalent to 7 km).  $K_s(z_t)$  and  $K_w(z_t)$  are the strong and weak weighting functions for the tangent level  $z_t$  (mentioned in the text) and  $z''$  is the approximate centre of  $K_s(z_t)$ .

weighting function here is defined by analogy with vertical sounding such that the observed radiance  $I = \int K(z) B(z) dz$ , where  $z$  is the pressure scale height. For the upper tangent levels the emission is seen to originate from layers slightly broader than the field of view, because the ray is close to the tangent level for a large part of the path. In these cases the atmosphere is optically thin, in that the tangent path is only partly absorbing. The total absorption ( $= 1 - \text{transmission}$ ) is also known as the emissivity  $\epsilon$  of the path, and is the area under the weighting function curve. Thus

$$I = \int_0^{\infty} K(z) B(z) dz = \overline{B(z_t)} \int_0^{\infty} K(z) dz = \overline{B(z_t)} \epsilon(z_t) \approx B(z_t) \epsilon(z_t), \quad (4)$$

where  $z_t$  is the tangent-point pressure scale height, and  $\overline{B(z_t)}$  is the Planck function averaged over the weighting function, hence approximately equal to the tangent-level value.

Consider the simplest case of a measurement in the wings of a Lorentz line through an optically thin atmosphere tangential to a fixed pressure level, at a single frequency where  $B \propto T^\beta$  and  $T$  is temperature. We have that  $\epsilon(z) \propto S(T) T^{-\gamma}$ , where  $S$  is the line strength, and  $\gamma$  is an exponent resulting from the temperature dependences of density, pressure scale height and Lorentz width and is normally about unity. Therefore  $I \propto S T^{\beta-\gamma}$ . In the mid-infrared  $\beta$  is typically 4, hence the measured radiance varies rapidly with temperature, unless  $S(T)$  happens to have a strong compensating inverse relation. In the microwave,  $\beta \approx 1$ , consequently the radiance measured is approximately independent of temperature, apart from any line strength dependence, and varies only with tangent pressure and gas-mixing ratio. This simplifies constituent sounding in the microwave, but makes temperature sounding rather difficult (see §6).

It is assumed that the instrument has two channels that measure in regions of differing opacity, but sufficiently close in wavelength that the Planck functions for a given temperature are equal. If both channels are optically thin we have:

$$I_w(z_t) = \epsilon_w(z_t) \overline{B(z_t)}; \quad I_s(z_t) = \epsilon_s(z_t) \overline{B(z_t)};$$

hence

$$I_w(z_t)/I_s(z_t) = \epsilon_w(z_t)/\epsilon_s(z_t) = f(z_t), \quad (5)$$

where  $w$  and  $s$  denote weak and strong absorption respectively;  $f(z_t)$  is mainly a function of tangent pressure and can be precomputed knowing the instrumental characteristics. Provided that  $f(z_t)$  varies with  $z_t$  monotonically and sufficiently rapidly, the ratio of measured radiances is sufficient to determine the tangent-level pressure for any collocated pair of measurements during the scan.

Suppose that this had been done, then  $\epsilon_w(z_t)$  or  $\epsilon_s(z_t)$  can be calculated, and  $\overline{B(z_t)}$  and the temperature derived. So far every level has been treated separately, and its pressure and temperature found. The mean temperature between tangent-level temperatures can be found quite independently by using the hydrostatic equation and the rate of change of pressure with height. Clearly the two derived temperature profiles need to agree, and the hydrostatic equation may be seen as a constraint upon the direct radiometric solution.

In practice,  $f(z_t)$  varies slowly (optically thin emissivity curves tend to vary with pressure such that they stay proportional to each other), so that this mechanism provides only marginal information about pressure registration. We will denote the above, mechanism (a).

The lower-altitude weighting functions are broader, and here the atmosphere is opaque (optically thick) and the emissivity is unity. In this case,  $\overline{B(z_t)} \neq B(z_t)$  because the radiation originates from a point closer to the satellite than the tangent point, similar to vertical sounding, hence at a greater altitude. Suppose that the strong channel is optically thick at a level where the weak channel is still optically thin (level  $z'_t$ ). Then  $\epsilon_s$  is unity, and  $I_s$  gives the value of the Planck function at a level  $z''$ , which is slightly above  $z'_t$ , but is insensitive to good knowledge of  $z'_t$ . Knowing the Planck function near  $z''$  it is now possible to find the pressure registration necessary to give the observed weak-channel radiances in the vicinity of this level. The scan has now been 'registered' in pressure at this level. It is now possible to integrate up and down the height scale from this level, deriving temperature, and by way of the hydrostatic equation using this to give the pressure at the next point. This we will call mechanism (b).

The above are conceptual methods of performing the retrieval. Methods actually used tend to be optimum numerically, but give little understanding of where the information arises, or indeed whether there is enough information for the measurements to specify the solution over and above the *a priori*. In the case of the SAMS, it appears that the information mainly arises from mechanism (b), but mechanism (a) with its hydrostatic constraint does have some effect.

The retrieval method employed for the SAMS was described in detail by Rodgers *et al.* (1984). It has a simple Kalman filter estimator assimilating radiance ratios as in mechanism (a) to find approximate tangent-level pressures as a linearization point, then a Kalman filter using all of the information to obtain profiles of temperature against pressure. These are then used in the retrievals of constituents. Inherent in the physics of the temperature and pressure retrieval is a repeated switch between pressure and height coordinates, but the primary coordinate is chosen to be pressure. The choice of coordinate system should be arbitrary provided that the

problem is formulated to represent adequately the information and constraints, although it can clearly have profound effects upon the computational difficulty.

The LRIR and LIMS retrieval methods were described by Gille *et al.* (1980), Gordley & Russell (1981) and Bailey & Gille (1986). They combined the radiances from adjacent pairs of scans, using the difference between the scans to allow for a linear rate of change of roll angle. The radiance profiles for the two channels were then retrieved by an iterative procedure, that was essentially a sophisticated version of mechanism (b) described above. Overall, the retrieval problem is highly nonlinear, so for both the SAMS, LRIR and LIMS it was helpful to use a robust algorithm to obtain an approximate result about which to linearize to simplify convergence of the final stage of the process.

In the case of *Nimbus 6* and *7*, the satellite-derived absolute heights are not sufficiently accurate to be useful, and if a temperature profile as a function of height is required it is necessary to tie it to a radiosonde-derived analysis in the lower stratosphere (accurate to a few hundred metres), or to a climatological height field at this level (accurate to a few kilometres).

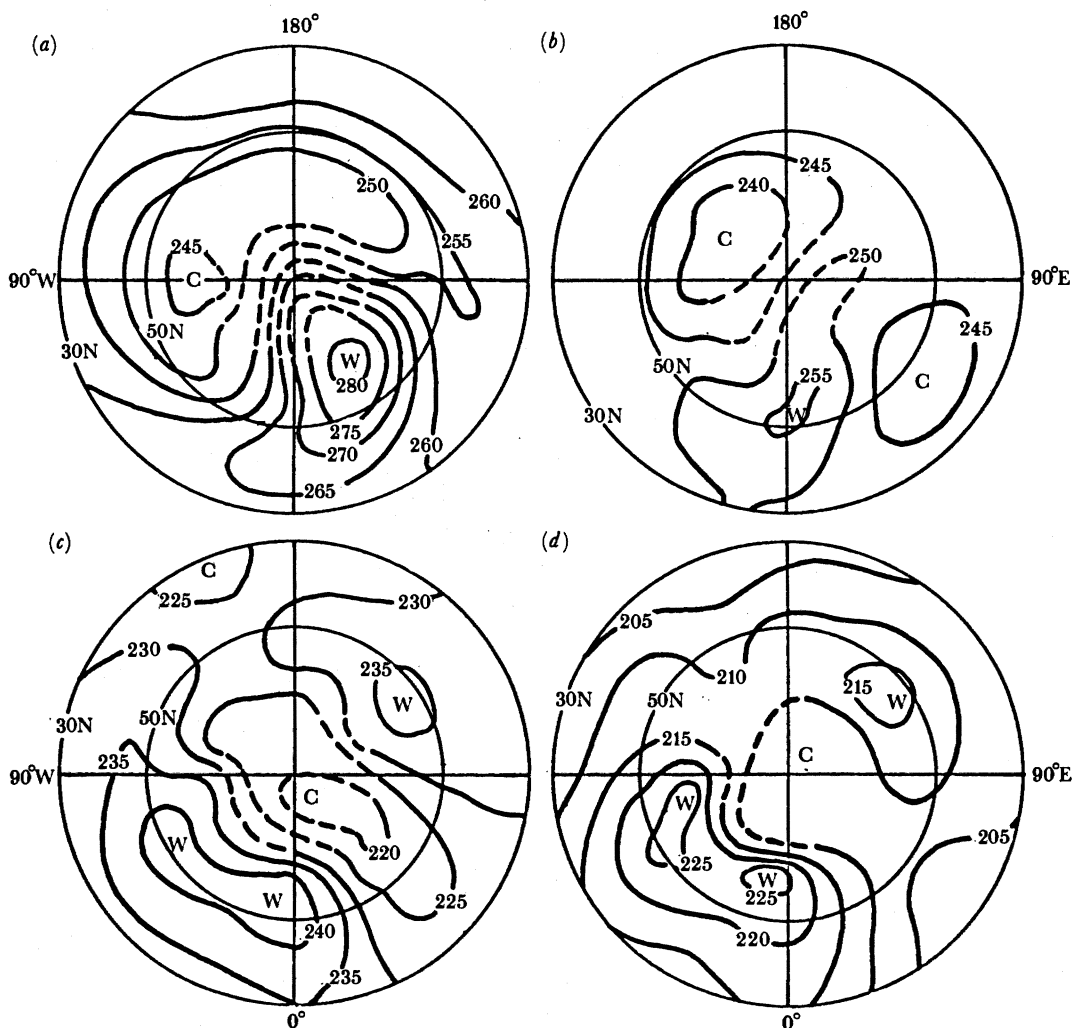


FIGURE 3. Temperature in the Northern Hemisphere retrieved from SAMS data for 27 February 1983 for the (a) 1, (b) 0.3, (c) 0.1 and (d) 0.03 mbar pressure levels.

Only if absolute heights are known better than this, implying elevation angle knowledge of arcseconds (for the SAMS,  $1' \approx 1$  km at the limb), can they make a useful contribution.

### 3.2. Results from limb sounders and comparison with vertical sounding

Figure 3 gives an example of temperature fields derived from the SAMS for the upper stratosphere and mesosphere during a stratospheric warming. Significant measurements are made up to about 0.03 mbar (70 km). The instrument made no measurements north of 70 °N, and the broken contours were obtained by interpolation, with the assistance of other measurements.

Intercomparison has been the subject of a series of workshops organized as part of Pre-MAP Project 1. The intention was to compare, for the same dates, fields from the LIMS, SAMS, the British Meteorological Office, the National Meteorological Center (NMC), the European Centre for Medium Range Weather Forecasting (ECMWF), and Berlin Free University. The NMC fields used VTPR data up to February 1979, and TOVS thereafter. The ECMWF gave analyses up to 30 mbar, based on many data sources including satellite, and Berlin gave fields up to 10 mbar based on non-satellite data (mainly radiosondes and rocketsondes). The British

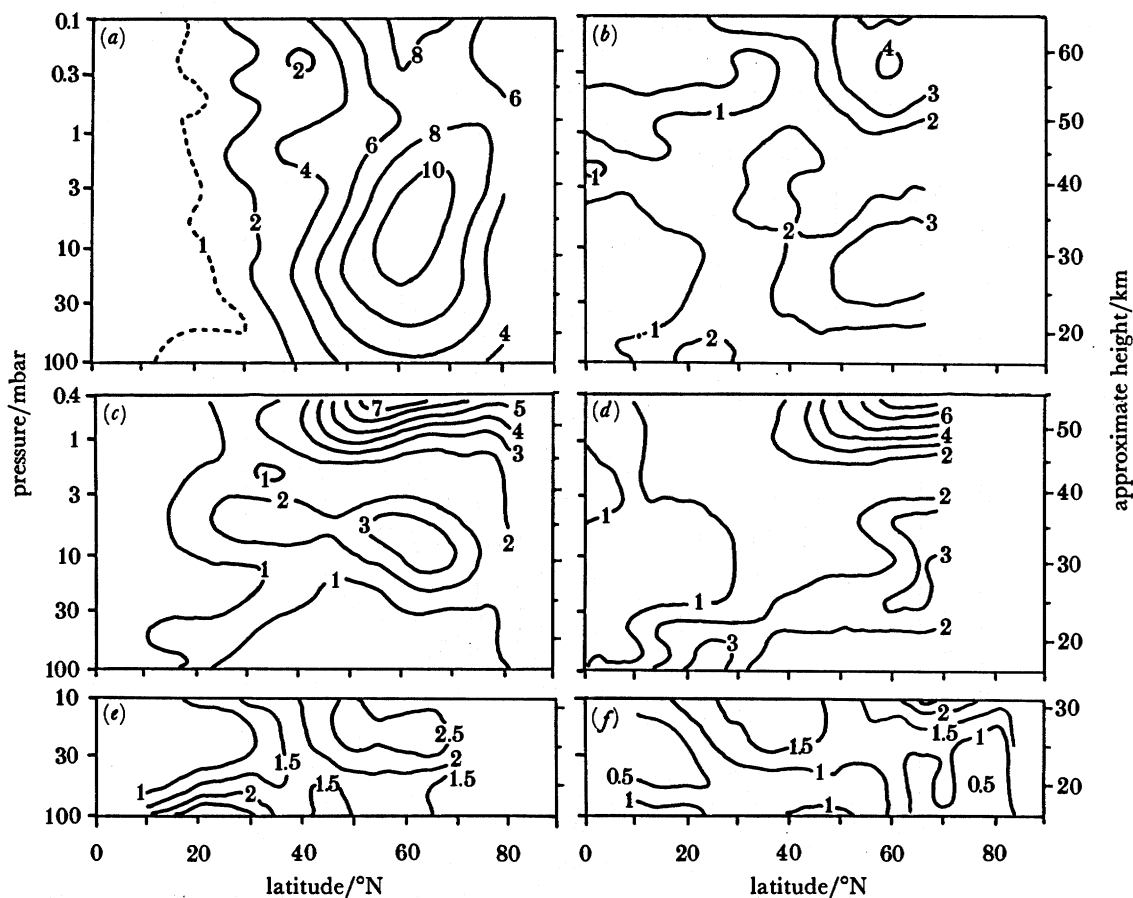


FIGURE 4. Comparison between different monthly mean fields of analyzed temperature for January 1979 (adapted from Rodgers 1984*b*). The height scale is approximate. (a) The r.m.s. LIMS variation around the Earth; (b–f) r.m.s. differences (averaged around the Earth) between: (b) SAMS and LIMS; (c) NMC and LIMS; (d) NMC and SAMS; (e) SAMS and the Berlin radiosonde analyses; (f) LIMS and the Berlin radiosonde analyses.

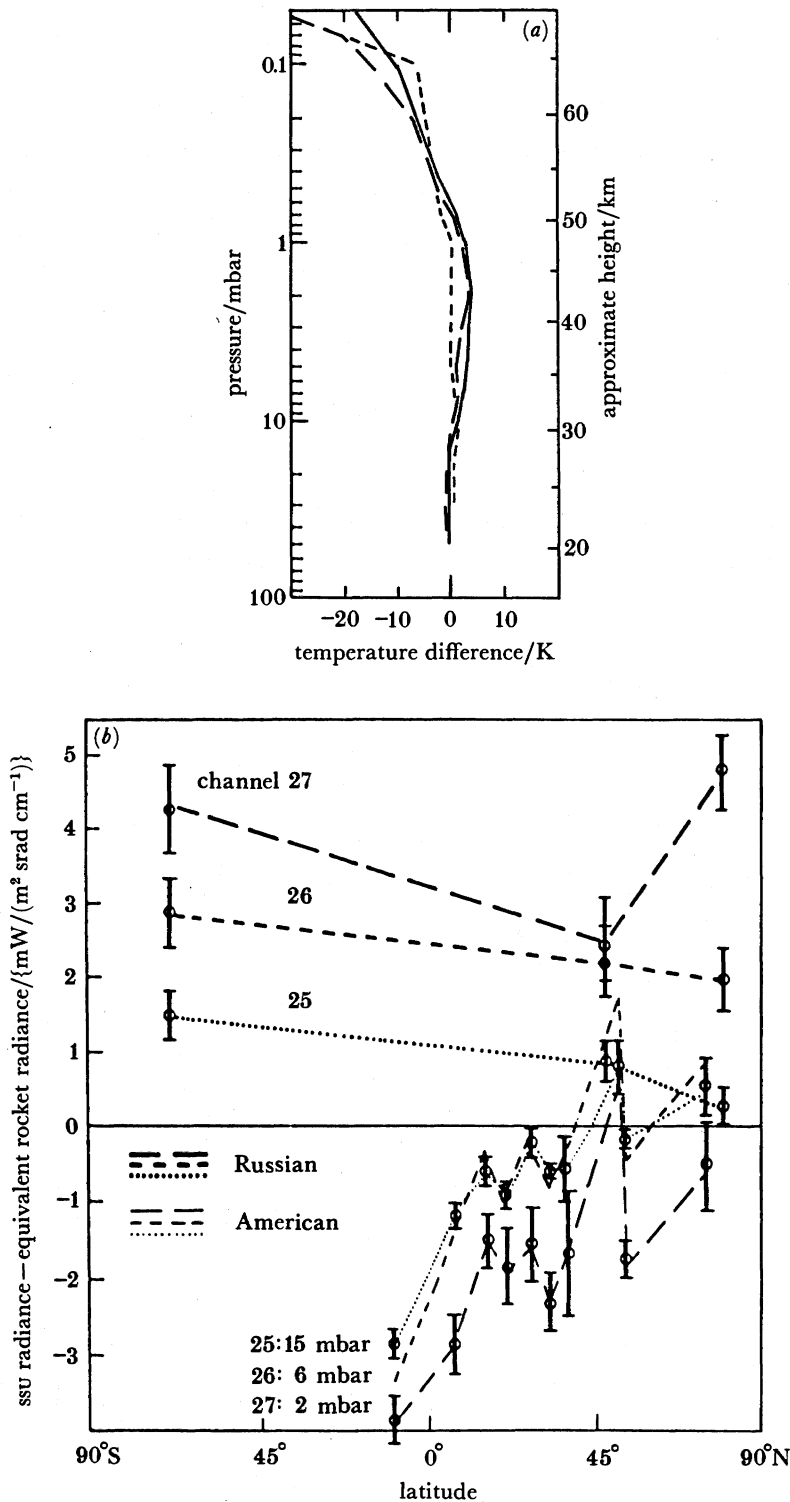


FIGURE 5. (a) Temperature difference between LIMS retrievals and U.S. datasonde rockets for zones: 10° S–11° N, ---; 47–57° N, ----; 75–83° N, ——. (Adapted from figures by Gille *et al.* 1984.) (b) Radiance difference between NOAA 6 ssu channels 25, 26 and 27, whose weighting functions peak near 15, 6 and 2 mbar respectively, and corresponding radiances calculated from U.S.S.R. and U.S. rocket temperature profiles (Nash & Brownscombe 1983). One radiance unit change corresponds very approximately to 1 K. In both (a) and (b) the value plotted is satellite–rocket.



Meteorological Office fields were based on data from the TOVS retrieved independently of the other groups. The work has been reported by Rodgers (1984 *a, b*) and Grose & Rodgers (1986).

Northern Hemisphere fields for single selected days and for monthly means were examined. Figure 4 gives an example of the comparisons for the January means. Figure 4*a* gives the standard deviation around latitude circles in the monthly mean measured by the LIMS; values of up to 11 K were found. Root mean square differences (after subtracting the zonal mean bias) between the SAMS and LIMS were typically 2–3 K (figure 4*b*). Similar differences are found between the other fields except that:

(*a*) fields based largely on radiosondes (e.g. ECMWF and Berlin) agreed with each other particularly well (they are based on the same basic measurements, but were subject to different transmission loss, editing and analysis procedures);

(*b*) NMC disagreed markedly with the LIMS and SAMS above about 1 mbar, which is above the peak of the highest VTPR weighting function.

A similar exercise was carried out for Southern Hemisphere fields in April 1986 (the report is still at the editorial stage). The conclusions are broadly in agreement with those for the Northern Hemisphere, but in addition it appeared that the tropospheric data used to specify the geopotential base-height was a major source of error for dynamical studies, particularly over Antarctica.

This kind of comparison is valuable in revealing problems, although it must be remembered that data-reduction methods are constantly evolving, and in the case of operational satellite instruments, it is often impractical to reanalyse old data sets with a new algorithm.

Comparison with *in situ* measurement methods has always been an important part of satellite instrument validation, and has been performed routinely with radiosondes and rocketsondes for the TOVS. In the case of vertical sounders there is a choice between (*a*) comparing radiances observed by the sounder with those calculated from the *in situ* temperature profile; (*b*) comparing the retrieved product. Figure 5 shows the result of such a comparison of radiance for the SSU channels. Marked biases that vary with latitude were found between the satellite and rocketsondes. These were in agreement with analyses performed during the previous year (Pick & Brownscombe 1981). Gille *et al.* (1984) gave corresponding comparisons for rockets with the LIMS retrievals, and found the same sign of latitudinal trend for the U.S. rockets, with the satellite becoming relatively hotter when further northward. Compared with U.S.S.R. rockets, both LIMS and SSU were markedly warmer. The cause of these biases is not known. However, the satellite in this case provides a valuable tool for intercomparing *in situ* measurements, so that they may be adjusted to give a single compatible result.

#### 4. PRESSURE SCALE-HEIGHT MEASUREMENT

The solar mesosphere explorer satellite launched in 1981 carries a visible light Ebert Fastie spectrometer whose primary purpose is to measure nitrogen dioxide concentration below 40 km. Above 40 km there is very little nitrogen dioxide absorption, and this enables temperature measurement in quite a different way. The satellite spins about an axis that is perpendicular to the orbit plane, with a period of 12 s. The direction of view is radial and so scans across the atmospheric limb twice per revolution, although data are only acquired for one of the scans. Two channels can be selected from the range 313–647 nm, and 439 and 442 nm are normally

used. Solar radiation, Rayleigh scattered by air molecules, is measured and this essentially provides a measure of the number of molecules along the tangent path. The altitude for unit optical thickness is about 23 km, and above about 28 km single scattering can be assumed. Hence there will be weighting functions analogous to those of a limb-emission sounder viewing at an optically thin wavelength. The field of view is about 3.5 km high at the limb. As with limb-emission sounding, the relative height scale is known more accurately than the absolute height. In this case absolute height is known to about one kilometre from horizon sensor information.

The method of retrieval can be demonstrated very simply. By the application of simple geometry and the hydrostatic relation, it can be shown that for a horizontally stratified atmosphere the number of molecules per unit cross sectional area of a tangent ray is proportional to  $pT^{-\frac{1}{2}}$ , where  $p$  is the tangent pressure and  $T$  is the temperature near the tangent level. Hence the scattered radiation  $I$  is given by

$$I(h) = Ap(h) T(h)^{-\frac{1}{2}}, \quad (6)$$

where  $h$  is height and  $A$  is a constant of proportionality related to the solar zenith angle, the wavelength, etc. Hydrostatic balance implies that  $Mg/RT = -d \ln p/dh$ , where  $M$  is the molecular mass of air,  $R$  the universal gas constant, and  $g$  the gravitational acceleration. Hence

$$d \ln I/dh + \frac{1}{2} d \ln T/dh = -Mg/RT. \quad (7)$$

Because the first term on the left-hand side will always dominate over the second, (7) may be solved iteratively (starting from an isothermal temperature profile), by obtaining an improved temperature on the right-hand side by using the measured  $I(h)$  and  $T(h)$  from the previous iteration. So far only relative values of  $I(h)$  have been used, and temperature has been found as a function of height, but no pressure information has been obtained. Given adequate absolute calibration, (6) may now be used to derive  $p(h)$  at all points of the scan. In practice, the SME data reduction is more complex than this, having to account for a finite field of view and scattering away from the tangent point. The method is described, together with results, by Rusch *et al.* (1983). By this technique they were able to derive temperature between about 40 and 50 km with about 3.5 km vertical resolution, and with r.m.s. deviations from nearby rocket soundings of 2–3 K below 45 km and 5 K above.

##### 5. SOLAR-OCCULTATION MEASUREMENTS OF TEMPERATURE

The atmospheric trace molecular spectroscopy experiment (ATMOS) is a Michelson interferometer (Farmer & Raper 1986) comparable in quality with the best found in laboratories, and was flown on Spacelab 3 on the Space Shuttle in April/May 1985. Although the instrument failed early in the mission, twenty occultation profiles were obtained for various wavelength ranges. The instrument locks onto a small part of the solar disc, and during sunrise and sunset measures a two-sided interferogram every 4 s, corresponding to a vertical spacing of about 4 km. Filters determined the overall band-pass, and these covered different ranges, e.g. filter 3 referred to later measured between 1580 and 3400  $\text{cm}^{-1}$ . For a given occultation, a single filter was always selected, and not changed. The vertical field of view could be varied but the minimum of 1 mrad (*ca.* 2 km) was used for filter 3.

The data have been studied by many groups. As with other temperature measurements,

species of known mixing ratio are used to determine the temperature and pressure. However, the ATMOS has the advantage of accurate absolute height knowledge (about 0.5 km or about 7% in pressure), so that it is reasonably satisfactory to use results on the ATMOS height scale, as opposed to a pressure scale derived from the data or a height scale derived by tying the pressure scale to a radiosonde analysis.

Figure 6 shows a small part of the carbon dioxide  $\nu_3$  band near  $2400\text{ cm}^{-1}$ . At pressures of 100 mbar or less the lines tend to be separated and in principle can be measured in such a way

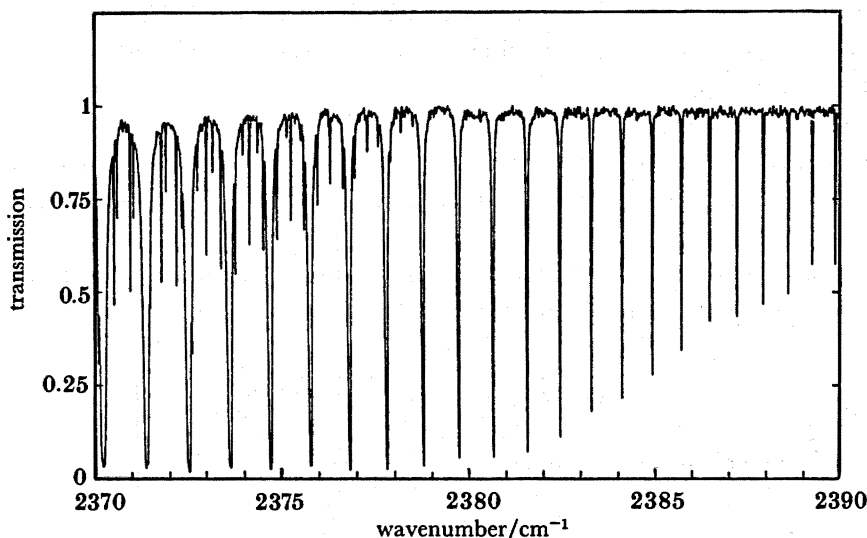


FIGURE 6. A small part of an ATMOS filter 3 ratioed spectrum taken during the sunset occultation on 30 April 1985 at  $30^\circ\text{ N}$ ,  $70^\circ\text{ W}$ , centred at 60.4 km tangent height. The spectral lines are primarily from the carbon dioxide  $\nu_3$  band. (From Muggeridge (1986).)

as to yield temperature and pressure information. The instrument resolution is of the order of  $0.01\text{ cm}^{-1}$  (depending on the operational mode). This is an order of magnitude greater than Lorentz line widths in the low stratosphere, and two orders of magnitude greater than Doppler widths. Various kinds of information are present in the data. Clearly the equivalent width (integrated area under the absorption curve) can be derived for an isolated line. In addition, for very broad lines, it may be possible to extract information about the line shape. Muggeridge (1986) used a selection of well-isolated lines from each interferogram. The equivalent width of each was obtained, having allowed for a slowly varying background due to strong distant lines. The equivalent widths were fitted by a nonlinear least squares method, to obtain the temperature and pressure profile that gave equivalent widths that most closely matched those measured. The equivalent width of a spectral line depends on pressure (because of Lorentz broadening), temperature (Lorentz and Doppler broadening, and strength) and density (or the number of molecules along the path). Density is itself related to the temperature and pressure by the gas laws. Lines were chosen that had a range of temperature line-strength dependence, so that from an interferogram it should be possible to derive effective temperature and pressure at the tangent point. As with limb sounding, the hydrostatic equation constrains the solution for a profile, because the relative heights of different paths during the scan are accurately known. However, the locus of tangent points is not in general vertical, so it is necessary to

assume horizontal stratification. Muggeridge formulated the equations in height coordinates, and estimated the vector

$$\left( \ln(p_0), \frac{1}{T_{k_1}}, \frac{1}{T_{k_2}}, \dots, \frac{1}{T_{k_n}}, \frac{1}{T_{v_1}}, \frac{1}{T_{v_2}}, \dots, \frac{1}{T_{v_n}} \right), \quad (8)$$

where  $p_0$  is reference pressure at some chosen height (80 km was used),  $T_k$  and  $T_v$  are the kinetic and vibrational temperatures, respectively, at every height level. From this vector the value of  $\ln(\text{pressure})$  at any height can be obtained by a linear operation, by using the hydrostatic relation. Consequently the problem can be linearized by calculating partial derivatives of the equivalent widths of each line at each observed level with respect to each component of the estimate vector.

Two kinds of result were obtained:

(a) kinetic temperatures between about 10 and 100 km, by using lines that result from a transition to the ground state, and that are consequently less dependent on non-local thermodynamic processes;

(b) kinetic and vibrational temperatures for the carbon dioxide  $v_2$  and  $2v_2$  levels between 60 and 110 km, based upon ground and higher-state transitions.

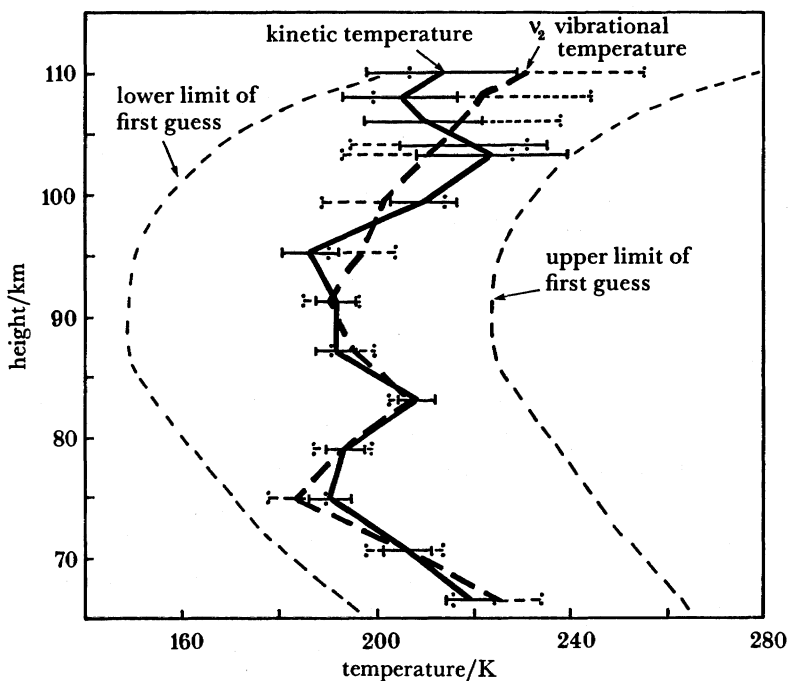


FIGURE 7. Kinetic temperature (solid line) and carbon dioxide  $v_2$  vibrational temperature (broken line) retrieved by Muggeridge (1986) from the ATMOS filter 3 sunset occultation at 17.25 GMT on 1 May 1985 at  $26^\circ$  N,  $14^\circ$  E. The height scale is that derived from the Space Shuttle orbital elements.

Figure 7 gives results for the latter case for one occultation. The vibrational and kinetic temperature are nowhere significantly different from each other. This is quite different from current theory, which implies that vibrational temperatures should be substantially lower than kinetic for these transitions above 80 km (López-Puertas *et al.* 1986). Muggeridge notes that a factor of 10 increase of the assumed atomic oxygen mixing ratio would allow the theory to agree, but there are many other ways in which agreement could be obtained.



## 6. FUTURE INSTRUMENTS

The *Tiros-N* series of operational sounders will continue to be launched during the 1980s, but in about 1990 the msu and the ssu will be replaced by the advanced microwave sounder unit (AMSU). This will be a quasi-vertical sounder, scanning across the track. There will be 20 channels, of which 6 of the temperature channels will have weighting functions peaking above 100 mbar (with the highest peaking at about 2.5 mbar). It will scan across the track and make stratospheric measurements at intervals of 50 km (30 samples across the swath). The instrument should give major improvements in tropospheric sounding, but the only advantage for stratospheric sounding will probably be in better vertical resolution, which will probably be about 10 km, compared with that of the ssu of about 12–15 km.

In 1991 NASA is due to launch the Upper-Atmosphere Research Satellite (*UARS*). This is a large satellite (mass 7500 kg), carrying nine instruments, devoted to the study of the upper atmosphere and its energy input from the Sun. There will be two infrared limb-emission sounders to measure temperature, in addition to many trace constituents.

(a) The improved stratospheric and mesospheric sounder (*ISAMS*); this will be an advanced version of the *SAMS*, with gas correlation to obtain improved spectral resolution. It will use detector arrays, cooled to 80 K by mechanical coolers (with an indefinite lifetime). The vertical field of view at the limb will be about 2.5 km.

(b) The cryogenic limb array etalon spectrometer (*CLAES*) will use a  $0.18\text{--}0.65\text{ cm}^{-1}$  bandwidth Fabry–Perot etalon spectrometer, able to scan across several  $3\text{--}12\text{ cm}^{-1}$  wide intervals in the range  $780\text{--}2900\text{ cm}^{-1}$ . The detector array will be cooled by a neon–carbon dioxide cryostat to less than 15 K; the spectrometer and optics will also be cooled. The cryogen lifetime is currently not clear, but will probably be about 21 months, assuming a 50% duty cycle. The detector vertical field of view will be 2.8 km.

The *UARS* will also carry the microwave limb sounder (*MLS*) that will measure microwave thermal emission from oxygen near 63 GHz, to determine the pressure level to enable the interpretation of other constituent-measuring channels. From measurements of pressure as a function of relative height, it may be possible to determine temperature by differentiation (from the pressure scale height), in a manner similar to that described in §4. In addition, the *UARS* will carry two other limb-viewing instruments to measure wind, from the Doppler shifts of spectral lines, and temperature from their Doppler widths. The wind imaging interferometer (*WINDII*) will be a Michelson interferometer, sensing airglow and aurora in the mesosphere and low thermosphere. The high-resolution Doppler imager (*HRDI*) will be a Fabry–Perot interferometer measuring atmospheric emission and scattered sunlight from levels between the upper troposphere and the lower thermosphere. Their noise levels will probably be substantially worse than those of the *ISAMS* and *CLAES* for individual profiles, but when averaged they should provide independent means of measuring temperature, without requiring the assumption of local thermodynamic equilibrium at the higher levels. The *UARS* was described in detail by the General Electric Company (1987).

In the longer term it is not clear how temperature sounding will progress. There is no obvious way to avoid simultaneously both the vertical resolution limits of vertical sounding, and the horizontal resolution limits of limb sounding. However, improved satellite stability and pointing knowledge may enable limb sounders to measure pressure on height surfaces to a better accuracy than the current radiosonde-based analyses provide. This might require the incorporation of a star tracker directly into the limb-viewing instrument, possibly sharing its optics



to eliminate some of the alignment drift problems. It would provide direct measurements of both the temperature and geopotential height fields in the middle atmosphere, and give much improved knowledge, particularly in the remote areas of the Earth.

## REFERENCES

- Bailey, P. L. & Gille, J. C. 1986 *J. geophys. Res.* **91**, 2757–2774.  
 Barnett, J. J. & Corney, M. 1984 *J. geophys. Res.* **89**, 5294–5302.  
 Barnett, J. J., Corney, M., Murphy, A. K., Jones, R. L., Rodgers, C. D., Taylor, F. W., Williamson, E. J. & Vyas, N. M. 1985 *Nature, Lond.* **313**, 439–443.  
 Drummond, J. R., Houghton, J. T., Peskett, G. D., Rodgers, C. D., Wale, M. J., Whitney, J. & Williamson, E. J. 1980 *Phil. Trans. R. Soc. Lond. A* **296**, 219–241.  
 Farmer, C. B. & Raper, O. F. 1986 High resolution infrared spectroscopy from space: a preliminary report on the results of the atmospheric trace module spectroscopy (ATMOS) experiment on Spacelab 3. In *NASA Conference Proceedings 'Spacelab 3 Mission Science Review'*, CP-2429 (ed. G. H. Fichtl), pp. 42–62. NTIS.  
 General Electric Company 1987 *UARS project data book*. Goddard Space Flight Center, Washington D.C.: NASA.  
 Gille, J. C., Bailey, P. L. & Russell, J. M. III 1980 *Phil. Trans. R. Soc. Lond. A* **296**, 205–218.  
 Gille, J. C. & House, F. B. 1971 *J. atmos. Sci.* **28**, 1427–1442.  
 Gille, J. C., Bailey, P. L. & Beck, S. A. 1984 *J. geophys. Res.* **89**, 11711–11715.  
 Gille, J. C. & Russell, J. M. III 1984 *J. geophys. Res.* **89**, 5125–5140.  
 Gordley, L. L. & Russell, J. M. III 1981 *Appl. Opt.* **20**, 807–813.  
 Grose, W. L. & Rodgers, C. D. 1986 *MAP handbook* **21**, 79–110.  
 Hanel, R. A. 1983 In *Spectrometric techniques* (ed. G. A. Vanasse), vol. 3, pp. 43–135. London: Academic Press.  
 Jones, R. L. & Pyle, J. A. 1984 *J. geophys. Res.* **89**, 5263–5279.  
 López-Puertas, M., Rodrigo, R., López-Moreno, J. J. & Taylor, F. W. 1986 *J. atmos. terr. physics* **48**, 749–764.  
 Miller, D. E., Brownscombe, J. L., Carruthers, G. P., Pick, D. R. & Stewart, K. H. 1980 *Phil. Trans. R. Soc. Lond. A* **296**, 65–71.  
 Muggeridge, A. M. 1986 *D.Phil. thesis*, University of Oxford.  
 Nash, J. & Brownscombe, J. L. 1983 *Adv. Space Res.* **2**, 59–62.  
 Nash, J. 1987 *Q. Jl R. Met. Soc.* (Submitted.)  
 Pick, D. R. & Brownscombe, J. L. 1981 *Adv. Space Res.* **1**, 247–260.  
 Rodgers, C. D. 1976 *Rev. Geophys. Space Phys.* **14**, 609–624.  
 Rodgers, C. D. 1984a *MAP handbook* **12**, 1–154.  
 Rodgers, C. D. 1984b *Adv. Space Res.* **4**, 117–125.  
 Rodgers, C. D., Jones, R. L. & Barnett, J. J. 1984 *J. geophys. Res.* **89**, 5280–5286.  
 Rusch, D. W., Mount, G. H., Zawodny, J. M., Barth, C. A., Rottman, G. J., Thomas, R. J., Thomas, G. E., Sanders, R. W. & Lawrence, G. M. 1983 *Geophys. Res. Lett.* **10**, 261–264.  
 Taylor, F. W. 1983 In *Spectrometric techniques* (ed. G. A. Vanasse), vol. 3, pp. 137–197. London: Academic Press.

## Discussion

S. A. BOWHILL. Can one shed light on the temperature discrepancy between the satellite and rocket techniques by computing the expected radiance from the rocket temperatures, rather than comparing the temperatures directly?

J. J. BARNETT. This method is frequently used and is extremely valuable for vertical sounders, because it avoids satellite retrieval errors. Nearly isothermal profiles give information about radiative calibration errors, and profiles with steep lapse rates can indicate atmospheric transmittance errors. For limb sounders, radiance profiles against relative scan angle can be calculated by assuming that the satellite attitude is not changing. However, for satellites with insufficiently controlled or known attitude (such as *Nimbus 7*), it is necessary to take into account the change of attitude during the scan. This is determined as a necessary part of the retrieval process, but to use the results to correct a calculated radiance profile would then render the comparison dependent upon the retrieval. This would seem to be no better than comparing retrieval temperature profiles, as is normally done.